Linear Velocities of Persistent Superfluid-Helium Currents and the Role of Vortex Lines*†

James C. Weaver‡
Department of Physics, Yale University, New Haven, Connecticut 06520
(Received 25 August 1971)

An investigation of superfluid-helium persistent currents in narrow annular channels is discussed, with an emphasis on the macroscopic linear superfluid velocity v_s. The channels have radial widths $d=R_2-R_1$ ranging from 8.20×10^{-1} to 8.45×10^{-1} cm, heights from 7.2×10^{-3} to 4.6 cm, and contain no porous filler material. The observed maximum persistent velocities are identified as the superfluid critical velocity $v_{s,c}$ and constitute the first direct measurements of the linear superfluid critical velocity. These experimental values of $v_{s,c}$ are in fair agreement with a simple theory which intimately involves vortex lines. This theory includes a dissipative superfluid critical velocity involving pinned vortex lines which is in over-all agreement with the previous models of Feynman and of Glaberson and Donnelly, but which is especially appropriate for rotational experiments with our geometry. Also, the critical angular velocity of Donnelly and Fetter for the disappearance of vortex lines is associated with the superfluid rather than the bucket in the case of (metastable) persistent currents. Furthermore, it is shown that normal-fluid turbulence was avoided in these measurements and that, therefore, the criticism of Van Alphen *et al.* does not apply. Nevertheless, the present results do not agree with the empirical Leiden formula. Finally, Andronikashvili's original attempt to observe persistent currents is reexamined. The over-all results of this work strongly support the involvement of vortex lines in superfluid critical velocities for the cases investigated.

INTRODUCTION

Critical velocities of superfluid helium have been a topic of both theoretical and experimental interest from almost the beginning of the study of superfluid helium, and there now exists a considerable literature devoted to it.[1] Originally a superfluid was defined to be a fluid which flows through channels without friction, but early experiments soon revealed that superfluid helium obeys this simple definition only for small velocities. Instead, above a certain velocity, the superfluid critical velocity $v_{s,c}$, dissipation sets in. Below $v_{s,c}$ the flow is believed to be genuinely frictionless and persistent flow is possible. The present work concerns the first direct measurements of the maximum linear persistent superfluid velocity for a number of different-size annular channels. Since the linear critical velocity $v_{s,c}$ is an upper bound for the linear persistent superfluid velocity v_s, this method provides a direct measurement of superfluid critical velocities. Some of the results have been briefly described previously.[2]

BASIC EXPERIMENTAL METHOD

The persistent superfluid velocities measured here are obtained by using a variation of methods developed previously.[3] A sealed container or "bucket" containing helium II is suspended from a magnetic bearing so that it can rotate almost frictionlessly about a vertical axis. Figure 1 shows the main features of an idealized bucket. No porous filler material is used in the bucket channels. Also, it is important to note that the dimensions of the channels in these buckets are such that velocity field of the superfluid is not likely to vary by much from $r=R_1$ to $r=R_2$. Specifically (see Appendix A) it is a good approximation to treat the macroscopic velocity field $v_s(r)$ as a simple constant, $v_s(r)=v_s$. This has the consequence that the superfluid persistent velocity v_s is simply related to the directly measured total angular momentum L_s of the persistent flow by

$$v_s = 3L_s/[2\pi N D\rho_s(R_2^3-R_1^3)]\,, \tag{1}$$

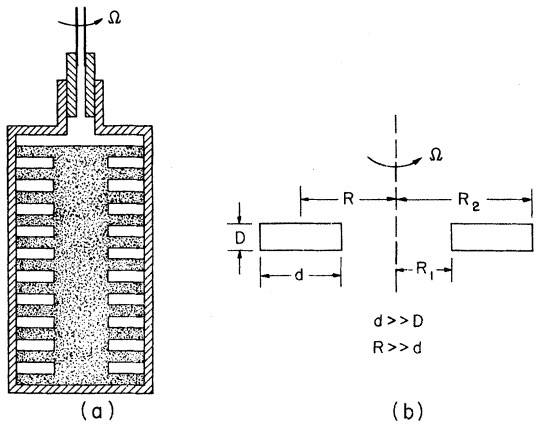

FIG. 1. (a) Cross section of a typical bucket showing the N identical channels (for illustration, N equals only ten). (b) Schematic of the cross section of a single channel showing the channel width $d=R_2-R_1$, height D, and mean radius R. With the exception of bucket VII, the conditions $D\ll d$ and $d\ll R$ were always satisfied.

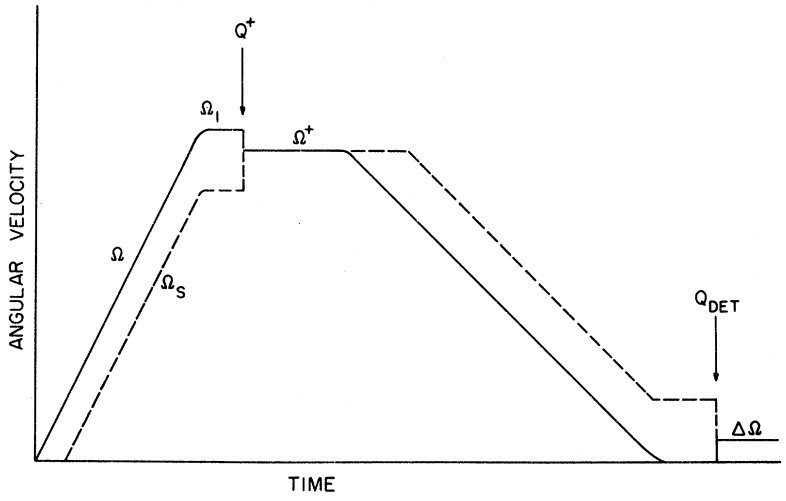

FIG. 2. Sequence comprising an Ω^+ run. The solid line indicates bucket angular velocity Ω (measured) and the dotted line indicates superfluid angular velocity Ω_s (inferred). A persistent current is created by forcing the superfluid into equilibrium at $\Omega = \Omega_s = \Omega^+$ by means of a heat pulse Q^+. Subsequent deceleration of the bucket to $\Omega = 0$ results in a superfluid persistent current which is detected by forcing equilibrium by means of a second heat pulse Q_{det}. Angular momentum is conserved and the resulting change in the bucket's angular velocity, $\Delta\Omega$, allows measurement of the angular momentum of the superfluid persistent current L_s. The angular deceleration from Ω^+ is sufficiently small so as to avoid normal fluid turbulence. A single run requires from $1\frac{1}{2}$ to 3 h.

where N is the number of identical channels in the bucket D, R_1 and R_2 are the channel dimensions shown in Fig. 1, and ρ_s is the superfluid density. The measurements of L_s were all made in the temperature range 1.2–1.5 °K, well below the λ-point region where superfluid critical velocities show a temperature dependence. Earlier work by Clow and Reppy[4] and others has shown that the ratio of L_s/ρ_s is independent of T in this temperature region

For a particular bucket the quantities N, D, R_1, and R_2 are known and fixed, so that if the temperature is determined (fixing ρ_s), then it remains to measure the angular momentum L_s of the persistent superfluid current in order to determine the linear persistent superfluid velocity v_s. The experimental sequence followed to create and measure L_s is described with the help of Fig. 2. For simplicity we assume that the normal fluid closely follows the bucket without turbulence (see Appendix B). Then we need only consider the superfluid and bucket. At $t = 0$ both the bucket (angular velocity Ω) and the superfluid (angular velocity Ω_s) are at rest. Exchange gas is present which holds the bucket temperature close to that of the bath. The bucket is now accelerated (solid line) until the bucket reaches some angular velocity Ω_1. Presumably the superfluid (dotted line) lags during this acceleration, since if the relative velocity of the superfluid to the bucket is less than $v_{s,c}$ no coupling can occur. Shortly (30 sec) after the bucket reaches Ω_1, a short (1-sec) radiant heat pulse Q^+ is delivered to the bucket which forces the superfluid into equilibrium with the bucket. The bucket and superfluid now rotate at a common angular velocity Ω^+, the creation angular velocity for the persistent current which is about to be created. (Note that conservation of angular momentum results in the bucket slowing down to Ω^+, while the superfluid is now rotating faster.) About five minutes are spent at Ω^+ while the superfluid begins cooling via the exchange gas. Then a slow (see Appendix B) angular deceleration α is begun which eventually (after $\frac{1}{2}$–$1\frac{1}{2}$ h) brings the bucket again to rest ($\Omega = 0$). During the deceleration the superfluid does not couple to the bucket unless the magnitude of the relative angular velocity $|\Omega_s - \Omega|$ exceeds $v_{s,c}R^{-1}$. Thus the superfluid at first remains at Ω^+ while the bucket decelerates, and is decelerated only if the velocity difference exceeds the linear critical velocity for dissipation, $v_{s,c}$. When the bucket again reaches $\Omega = 0$, a second waiting period (well in excess of the damping time for the normal fluid) occurs, and then a second radiant heat pulse Q_{det} is applied which again forces equilibrium so that the bucket and superfluid rotate at a common angular velocity. The small (10^{-3} rad sec^{-1}) change in the bucket's angular velocity $\Delta\Omega$ is measured and allows a simple and direct determination of the superfluid persistent angular momentum L_s, since both the bucket's moment of inertia I and liquid moment of inertia I_s are known. Equation (1) now allows the linear superfluid persistent velocity to be readily determined. Data for a number of such sequences (runs) are plotted for each bucket as shown in Figs. 4–6. Both clockwise (upward pointing triangles) and counterclockwise (downward pointing triangles) measurements were made, with no noticeable difference between them.

Although most runs were made by the Ω^+ method shown in Fig. 2, a few runs were made in which the superfluid was dragged into rotation from rest. The experimental sequence followed for a drag run is indicated in Fig. 3. Again we focus our attention on just the bucket and superfluid. At $t = 0$ the bucket is at rest. Then, to ensure that the superfluid also

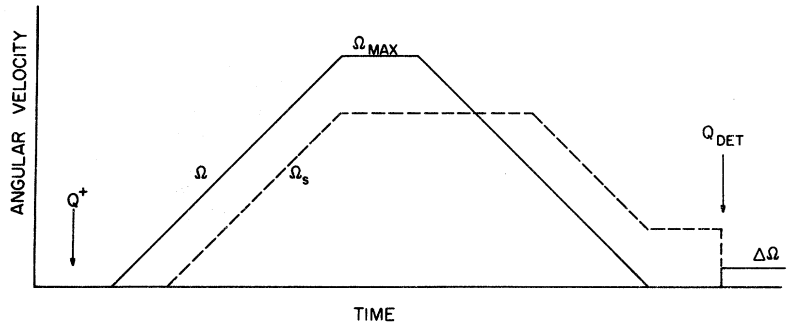

FIG. 3. Sequence comprising a "drag" run is shown. In this case the superfluid is dragged into rotation from rest in order to create a persistent current at $\Omega=0$. An initial heat pulse Q^* insures that the superfluid starts from rest, and the acceleration to and deceleration from Ω_{max} avoids normal-fluid turbulence. As in ordinary Ω^+ runs, the resulting current is detected and measured by means of a second heat pulse Q_{det} at $\Omega=0$. For a given bucket a drag run should generate a current less than those obtained by Ω^+ runs for all Ω_{max} up to $\Omega_{max}=2v_{s,c}R^{-1}$, provided $v_{s,c}$ is itself independent of Ω.

starts from rest, a radiant heat pulse Q^+ is delivered to the bucket so that the bucket and superfluid achieve a common velocity which is very close to zero. After a waiting period (5 min), the bucket is gently accelerated, and the acceleration is slowly reduced as Ω_{max} is approached. In drag runs no heat is applied at Ω_{max}. Instead, a second waiting period (5 min) is used during which the bucket rotates steadily at Ω_{max}. Then a gentle deceleration α is slowly turned on, and the bucket is eventually (after $\frac{1}{2}$–$1\frac{1}{2}$ h) returned to rest. Once again a second radiant heat pulse Q_{det} is applied to the bucket which forces equilibrium, so that the bucket and superfluid rotate at a common angular velocity. The resulting change in the bucket's angular velocity $\Delta\Omega$ is measured and allows determination of L_s and then v_s as is done for the Ω^+ runs. The data for these drag runs are also shown in Figs. 4–6, and were made for both clockwise rotation (circles) and counterclockwise rotation (squares). Note that for drag runs the measured value of L_s should be zero for all $\Omega_{max}<v_{s,c}R^{-1}$.

The measured superfluid critical velocity $v_{s,c}$ for each bucket is obtained by considering L_s as a function of Ω^+. For a given bucket the magnitude of L_s at first increases as Ω^+ increases, but then a plateau occurs for which L_s is constant. This maximum value of L_s allows calculation of the maximum persistent superfluid velocity $v_{s,max}$ by Eq. (1). But since $v_{s,c}$ is defined to be the superfluid velocity at which superfluid friction sets in, it follows that $v_{s,c}$ is an upper bound for the persistent superfluid velocity. Thus we make the identification $v_{s,max}=v_{s,c}$, and determine the superfluid critical velocity for each bucket from

$$v_{s,c}=3L_{s,max}/[2\pi ND\rho_s(R_2^3-R_1^3)]\,. \qquad (2)$$

The values for $v_{s,c}$ obtained by this method are presented in Table I.

APPARATUS

The apparatus used for these measurements is a variation and extension of one developed by Reppy and Depatie.[3] A schematic of the entire apparatus is shown in Fig. 7. In addition to the usual Dewars and liquid-helium bath, there is a central vacuum

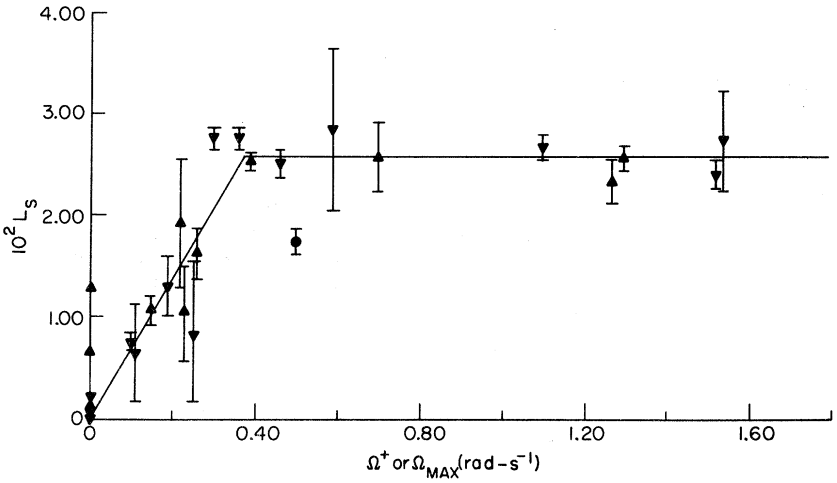

FIG. 4. Measured values of L_s as a function of Ω^+ or Ω_{max} for bucket II. All of the currents but one were made by the Ω^+ method. Upward pointing triangles (cw rotation) and downward pointing triangles (ccw) are for runs with Q^+; circles (cw) and squares (ccw) are for drag runs. The single drag run has $\Omega_{max}<2v_{s,c}R^{-1}$ and has $L_s<L_{s,max}$. The solid curve is obtained by first averaging the values of $L_{s,max}$ in the plateau region, and then making the linear rise consistent with this average value of $L_{s,max}$.

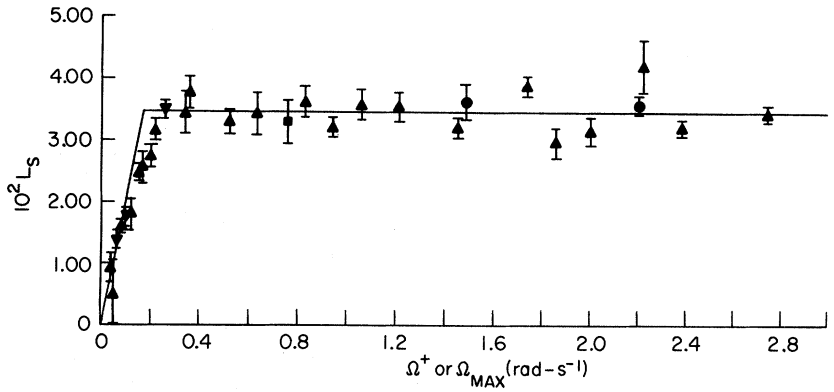

FIG. 5. Measured values of L_s for bucket III. The data for this bucket contain less scatter than any of the others, and this may possibly be due to the near equality of $R\Omega_0, v_{s,c}, v$ and the experimental critical velocity $v_{s,c}$.

region in which the magnetically suspended bucket rotates. During most of a run this vacuum region is filled with helium exchange gas which maintains the bucket at a low (1.2–1.5 °K) temperature. Although exchange gas is present for the application of heat Q^+ used to create a persistent current, the exchange gas is always pumped out just prior to detecting a persistent current. This is done to avoid convective torques on the bucket due to heating the exchange gas when the radiant heat pulse Q_{det} is applied. Such torques can easily cause spurious angular velocities which obscure the small change in bucket angular velocity $\Delta\Omega$, which is associated with the forced destruction of the persistent current. Measurements made on empty buckets after the exchange gas has been pumped out show only negligible torques. Typically five minutes are required to reach 10^{-5} Torr in the vacuum region before detection, and during this time the bucket's temperature slowly rises, but not excessively, and is duly noted.

The buckets are filled at the beginning of a series of runs by condensation through a one-meter-long stainless-steel filling tube which is also used for bucket temperature measurements during control runs. Once the bucket is filled and sealed off an entire series of runs is made, with the bath being replenished approximately every 22 hours. The bucket is suspended by the use of a "constant current" magnetic bearing which suspends a $\frac{1}{4}$-in. soft-iron sphere at the upper end of the vacuum region and from which the filling tube and bucket hang.[5] The upper end of the suspended bucket system is at room temperature and also contains the mirrors which are used for measuring the bucket's angular velocity. Below the mirrors hangs the one-meter length of $\frac{1}{32}$-in. stainless-steel thin-walled tube, with the bucket located on the lower end. Angular acceleration of the bucket is accomplished by applying a slipping rotating magnetic field to the iron sphere. In order to achieve lateral vibration isolation, the magnet for the magnetic bearing is mounted on a massive platform which is suspended from the ceiling by low-Q, humidity-insensitive fiber-glass ropes.

All buckets utilized identical magnesium outer shells, while the N identical annular channels were made in two ways. Buckets I, III, and IV were made

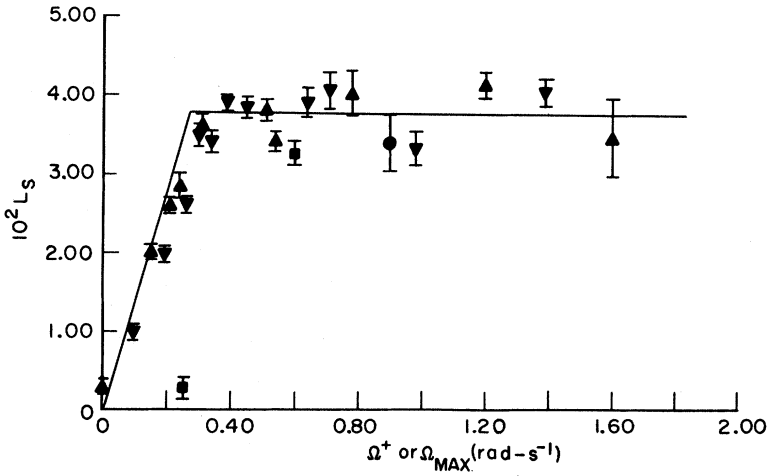

FIG. 6. Measured values of L_s for bucket VI which should have a critical velocity $v_{s,c}=R\Omega_0$. Note that the single drag run made with $\Omega_{max}<v_{s,c}R^{-1}$ yielded $L_s\approx 0$ as expected, whereas two drag runs made at higher Ω_{max} gave maximum L_s as expected.

TABLE I. Summary of data and bucket parameters. The various bucket channel dimensions are defined in Fig. 1. $v_{s,c,v}$ is the dissipative critical velocity involving pinned vortex lines and is given by Eq. (6). $R\Omega_0$ is the velocity below which vortex lines do not exist [see Eq. (7)]. The theoretical $v_{s,c}$ is the larger of $v_{s,c,v}$ and $R\Omega_0$, while the observed $v_{s,c}$ is the experimental result. Finally, $v_{s,c,l}$ is the empirical Leiden critical velocity given by Eq. (8).

Bucket	10^2D (cm)	10^1d (cm)	10^1R (cm)	$10^1v_{s,c,v}$ (cm/sec)	$10^1R\Omega_0$ (cm/sec)	Theoretical $10^1v_{s,c}$ (cm/sec)	Observed $10^1v_{s,c}$ (cm/sec)	$10^1v_{s,c,l}$ (cm/sec)
I	0.72 ± 0.20	1.59	8.20	2.8	1.6	2.8	3.2 ± 1.2	34
II	1.20 ± 0.14	1.60	8.21	1.7	1.6	1.7	3.0 ± 0.2	31
III	1.65 ± 0.28	1.59	8.20	1.3	1.6	1.6	1.4 ± 0.3	28
IV	3.35 ± 0.20	1.59	8.20	0.67	1.6	1.6	1.3 ± 0.3	23
V	5.00 ± 0.30	1.60	8.21	0.46	1.6	1.6	1.8 ± 0.5	21
VI	3.85 ± 0.20	1.30	8.35	0.59	2.5	2.5	2.2 ± 0.3	23
VII	4.60×10^2	1.09	8.45	0.0066	3.5	3.5	2.6 ± 0.9	17

by bonding together alternate glass discs (radius R_2) and Mylar discs (radius R_1 and thickness D). For buckets II, V, VI, and VII, the channels were machined from a solid magnesium cylinder which was subsequently inserted into the shell. In all cases the top of the bucket shell was sealed by an indium O ring, and the completed bucket whose top contained a small brass adapter was soft soldered to the filling tube.

Small mirrors were mounted on the rotating system slightly below the $\frac{1}{4}$-in. iron sphere. For all angular velocities except those close to zero, the angular velocity of the bucket was measured by reflecting a light beam from the mirrors and measuring the transit time of the reflected light between two photocells. However, for the low angular velocities encountered when measuring the $\Delta\Omega$ associated with Q_{det}, a different technique was used. Again one of the mirrors was used, but the reflected light was now focused on an oscillograph, and a trace of angular position as a function of time was thereby obtained so that the angular velocity could be subsequently calculated. The radiant heat pulse Q_{det} or Q^* was applied by using a quartz-iodine lamp operated from a Variac. As a prelude to real data taking, a series of Q_{det} selection runs was made for which $R\Omega^*$ was made much larger than the expected linear superfluid critical velocity, so that the same maximum persistent current was always expected. By trying a number of increasing levels of Q_{det} (which nevertheless gave a negligible $\Delta\Omega$ with still other runs for which $\Omega^*=0$) on this maximum current, we were usually able to find a satisfactory level of Q_{det} (the exceptions are possibly bucket I and certainly bucket VII). Since in these Q_{det} selection runs we could expect a maximum persistent current to be present, the measured angular momentum L_s at first increased with increasing Q_{det} but then saturated. We took saturation to mean that the complete angular momentum was being detected. Also, one complete series of regular runs was made with Q_{det} less than that which gives saturation, and the scatter in this data (L_s as a function of Ω^*, this data not shown) was much worse than usual. Finally, it is interesting to note that in most cases the final temperature of the bucket (after Q_{det}) was less than T_λ. As originally noted by Depatie,[6] if a long (several seconds) heat pulse Q_{det} is used to destroy the persistent flow by heating all the way to T_λ, all of the angular momentum is recovered in approximately the first one-tenth second. Possibly the mechanism for the rapid destruction of persistent superfluid flow is the generation of a second sound shockwave or turbulent counter current flow which causes equilibrium to be reached quickly.

It should be noted that it is not clear *a priori* that for a given bucket it will be possible to find a region of saturation as Q_{det} is increased. For some buckets, for example, still larger Q_{det} will cause a large spurious angular impulse in one direction. This effect seems to be a transient, and occurs only with buckets filled with liquid helium. This transient is probably due to exceeding T_λ in some of the chan-

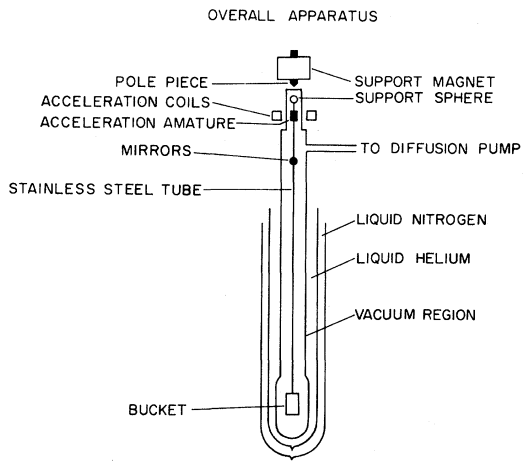

FIG. 7. Schematic of the entire apparatus. The essential features are briefly described in the text, and a more complete description is available in Ref. 3.

nels which causes boiling. Since it appears that more heat is necessary to destroy a current with a large persistent velocity than a small one, it is possible that for a bucket with a critical velocity above a certain value that the local boiling level can be reached before complete destruction of the current is obtained. This problem probably occurred with bucket VII and possibly with bucket I, since in both cases there was evidence of spurious angular impulses with the relatively large values of Q_{det} which appeared to be necessary even though $\Omega^+ = 0$. Also the data for bucket I have more scatter than the others, and this is consistent with Q_{det} being too small.

DATA

The data for several buckets are shown in Figs. 4–6, and the critical velocities derived from all buckets by use of Eq. (2) are presented in Table I. In all cases L_s initially increases, but at $\Omega^+ = v_{s,c}R^{-1}$, the persistent angular momentum reaches a maximum $L_{s,max}$. In determining $v_{s,c}$ from Eq. (2), only Ω^+ runs are used, and the few drag runs are excluded. Also, it should be noted that the break in the data at $\Omega^+ = v_{s,c}R^{-1}$ is not used to determine $v_{s,c}$, since the fractional errors in L_s and Ω^+ are larger for small Ω^+. However, this break is always found to be consistent with the value of $v_{s,c}$ which is determined from the value of $L_{s,max}$.

The error bars shown in Figs. 4–6 are rms estimates of the effect of measurements error on L_s. There are measurement errors in ρ_s/ρ owing to uncertainties in the bucket temperature, errors in the length measurements used to determine the oscillograph position, and in the length measurements made on the oscillograph record of angular position as a function of time which allow determination of $\Delta\Omega$. For most of the buckets the scatter was not much greater than expected from these estimated measuring errors. This indicates that in spite of the metastability of persistent currents and the existence of some vibration in the apparatus, persistent currents can be made fairly reproducibly. Only for buckets I and VII was there considerable excess scatter, and this, as was mentioned earlier, may be due to spurious effects associated with the large values of Q_{det} which were required for these buckets.

PINNED-VORTEX-LINE DISSIPATIVE CRITICAL VELOCITY

We find that our results are in agreement with a simple theory which intimately involves vortex lines in two ways: (i) a critical velocity for a dissipative mechanism involving pinned vortex lines, and (ii) an angular velocity below which vortex lines do not exist, thus shutting off the dissipative mechanism. We first discuss (i).

The first model for superfluid critical velocities which involved vortex lines was proposed by Feynman in 1955 and applies to a two-dimensional slot of width D which opens into a wide volume.[7] The mechanism for dissipation of the superfluid flow is the generation of a double train of vortex lines, and the Feynman model predicts that dissipation first begins when the superfluid velocity reaches

$$v_{s,c,f} = (k/2\pi D)\ln(D/a_0) , \tag{3}$$

where $k = h/m$ is the quantum of circulation, and $a_0 = 1.3\times10^{-8}$ cm.[8] More recently (1966) Glaberson and Donnelly have treated the case of a circular tube containing preexisting vortex lines pinned within a tube of diameter D.[9] They argue that if the bulk superfluid flow velocity through the tube is increased from zero, then the vortex line will grow and bend, and that such growth is stable only up to a critical radius. Above this radius the line grows unimpeded, and the removal of energy from the bulk superfluid flow by this mechanism allows an expression for the critical velocity to be obtained:

$$v_{s,c,gd} = (k/2\pi D)\left[\ln(4D/a_0) - \tfrac{1}{4}\right] . \tag{4}$$

A third simple model, more relevant to our experiment, applies to vortex lines pinned between two planes.[10] In this case, we consider two planes perpendicular to an axis of rotation as shown in Fig. 8. We assume that whatever changes are made in Ω, the angular velocity of the planes, are made so slowly that the normal fluid follows the planes without turbulence. Then we only need consider the superfluid component. Suppose that the system is rotating at Ω and that we have forced equilibrium to occur. From the Onsager-Feynman theory we then expect an array of vortex lines which are straight and parallel to the axis of rotation. Let us now examine what happens as we depart from equilibrium by slowing the rotation of the planes. We will assume that Ω is low enough to neglect centripetal effects and will simply ask what happens as the relative macroscopic velocity of the superfluid to the planes is increased from zero. That is, we will treat the problem for which initially straight vortex lines are present and pinned between the planes, and study what happens as the macroscopic superfluid velocity is increased from zero with respect to the planes. For simplicity, we will

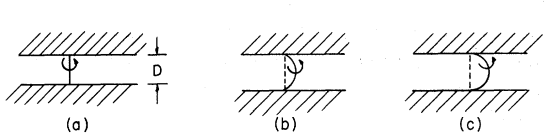

FIG. 8. Geometry for the derivation of Eq. (6). (a) shows an isolated vortex line pinned vertically between two infinite horizontal planes. (b) and (c) show the vortex line curved in a circular arc as the approximate result of an applied macroscopic velocity into the paper.

consider a single isolated vortex line as shown in Fig. 8(a). Initially the applied macroscopic superfluid velocity (i.e., that other than the velocity field of the vortex line itself) is zero and the pinned vortex line is straight as shown. Then as the applied velocity is increased (into the paper) the vortex line bends into a circular arc with radius $R > \frac{1}{2}D$, as shown in Fig. 8(b). This bending may be understood by appealing to the Magnus force $\vec{f} = \rho_s \vec{v}_s \times \vec{k}$, where $\vec{v}_s = \hat{\theta} v_s$ is the applied (locally constant) velocity and $\vec{k} = \hat{k}(h/m)$ is the vector circulation associated with a singly quantized vortex line. The vortex line tension (energy per length) $\vec{\epsilon}$ varies in direction in the same way as $\vec{k}$, and has a magnitude which is approximately

$$\epsilon = (\rho_s k^2/4\pi) \ln(D/2a_0) . \quad (5)$$

Here we have somewhat arbitrarily used one-half the plane separation as the cutoff for the velocity field of the vortex line. We neglect both self-Magnus forces and image attractions to the planes, assume that the ends of the line are pinned, and then find that the vortex lines assume a circular curve of radius $R \approx \epsilon/v_s \rho_s k$. It is postulated that the bending of the vortex line proceeds until $R = \frac{1}{2}D$ [Fig. 8(c)], at which point the vortex line is swept away, removing energy. The applied velocity v_s at which this occurs can be identified as the critical velocity $v_{s,c,v}$, and leads directly to

$$v_{s,c,v} = (k/2\pi D) \ln(D/2a_0) . \quad (6)$$

This result is in good agreement with the Feynman and Glaberson-Donnelly models. More significantly, it is also in agreement with the present rotational experiments for those cases in which persistent currents should contain vortex lines.

Ω_o OF DONNELLY AND FETTER

In addition to the preceding model for a linear critical velocity for the onset of superfluid dissipation, a calculation by Donnelly and Fetter is also relevant to our experiments, since this calculation determines an angular velocity Ω_o below which the existence of vortex lines is unfavorable.[11] Ω_o is the superfluid-helium analog of H_{c2} for type-II superconductors. In our notation this angular velocity is

$$\Omega_o = (k/\pi d^2) \ln(2d/\pi a_0) . \quad (7)$$

The calculation of Ω_o considers the equilibrium free energy for a two-dimensional case, therefore, contains no D dependence, and assumes straight rather than curved vortex lines. For (7) to hold, $d \ll R$. Although persistent currents are metastable rather than the equilibrium states for which this calculation applies, we nevertheless find that Ω_o can apparently be applied to the superfluid (rather than the bucket) for the persistent currents generated by our methods and which presumably contain curved rather than straight vortex lines.

INTERPRETATION OF RESULTS

We find that our experimental results can be understood in terms of the following theory. Suppose we consider a bucket with channels such that (i) $D \ll d$ (so that $v_{s,c,v}$ applies), (ii) $d \ll R$ (so that Ω_o governs the presence of vortex lines), and (iii) $v_{s,c,v} < R\Omega_o$. We begin by supposing that the superfluid has been forced into equilibrium with the bucket at some value of $\Omega^+ > \Omega_o$. After initially rotating at Ω^+ the bucket is decelerated slowly and the superfluid initially lags the decelerating bucket. Only when the relative linear velocity of the superfluid reaches $v_{s,c,v}$ can kinetic energy be removed from the superfluid flow, and when this dissipative process sets in, work is done as the vortex lines are swept radially outward, with eventual destruction of the vortex lines at the outer wall. However, if $\Omega_s > \Omega_o$, it is still favorable to create more vortices at the inner radius, and the dissipative coupling to the superfluid can be continued by supplying new vortices. However, when Ω_s falls below Ω_o it is no longer favorable to create new vortices and the mechanism for dissipation vanishes. If the bucket's deceleration is continued until $\Omega = 0$ a persistent current with velocity $v_s = R\Omega_o$ will then exist, and this is a maximum value. Thus, for the case in which the inequality $R\Omega_o > v_{s,c,v}$ holds, an irrotational (no vortex lines present) persistent current will exist at $\Omega = 0$, and the magnitude of the maximum persistent velocity will be $v_{s,\max} = R\Omega_o$.

On the other hand, suppose the channel dimensions are still such that (i) $D \ll d$ and (ii) $d \ll R$, but now (iii) $v_{s,c,v} > R\Omega_o$. Again let us imagine that the superfluid has been forced into equilibrium with the bucket at $\Omega^+ > \Omega_o$ and that subsequently a slow deceleration is begun. As before, only when the relative linear velocity of the superfluid reaches $v_{s,c,v}$ can kinetic energy be removed from the superfluid flow, and this dissipation occurs in the manner described previously. However, as the bucket is decelerated until $\Omega = 0$ the superfluid does not reach Ω_o since $v_{s,c,v} > R\Omega_o$. This means that the maximum persistent superfluid velocity will be $v_{s,\max} = v_{s,c,v}$ and that the persistent current contains pinned (but curved) vortex lines, even though the bucket is no longer rotating. Mutual friction cannot be invoked since the normal-fluid and vortex-line cores are both at rest with respect to the bucket, and the superfluid can, therefore, continue to flow in a genuinely persistent mode.

In short, this simple theory predicts two different types of persistent flow at $\Omega = 0$. If $v_{s,c,v} < R\Omega_o$, the persistent currents are vortex free or irrotational and their maximum linear velocity is $R\Omega_o$. On the other hand if $v_{s,c,v} > R\Omega_o$, the persistent cur-

rents contain pinned, although curved, vortex lines, and the maximum linear velocity is $v_{s,c,v}$ as given by (6). As shown in Table I, where the theoretical values are determined by this approach, the experimental values of $v_{s,\max}$ are in fair agreement with this theory.

LACK OF NORMAL-FLUID TURBULENCE

In 1966 Van Alphen *et al.* criticized a number of previous critical velocity experiments whose data were consistent with vortex-line models on the grounds that normal-fluid turbulence had occurred, and that this turbulence was mistaken for an onset of superfluid dissipation.[12] An alternate empirical formula for critical velocities, the Leiden critical velocity $v_{s,c,l}$, was also then proposed:

$$v_{s,c,l} = CD^{-1/4}; \quad C \approx 1 \text{ cm}^{5/4}\text{sec}^{-1} . \tag{8}$$

The previous experiments which were criticized did not involve direct measurements of persistent superfluid flow. Instead, they typically involved the forced flow of helium II (both ρ_n and ρ_s) through various types of channels, and determined the velocity at which dissipation of this flow first occurred. Nevertheless, it is possible that normal-fluid turbulence can couple to a persistent current. We can show, however, that normal-fluid turbulence was absent in our experiment (except for possibly bucket VII) by treating the case of a viscous incompressible fluid of density ρ_n which exists between two infinite parallel planes of separation D. Initially both the fluid and planes are envisioned to be moving at a constant common velocity $v^* = \Omega^* R$. Then at $t = 0$ a constant linear deceleration $a = \alpha R$ is turned on. Qualitatively we expect that the viscous fluid will lag the decelerating planes. Using several worst-case assumptions (Appendix B) we find that the maximum relative velocity $v_{n,\max}$ of the fluid to the planes is a constant, a terminal relative velocity of magnitude:

$$v_{n,\max} = \alpha R D^2/8\nu , \tag{9}$$

where ν is the kinematic viscosity. We make a conservative worst-case estimate of the maximum allowable angular deceleration $\alpha_{\max}$ in our experiment which avoids normal-fluid turbulence, and find

$$\alpha_{\max} = 8R_c \nu^2/RD^3, \tag{10}$$

where for parallel planes the Reynolds number R_c for the onset of turbulence is 10^3 or more,[13] and the minimum value of ν is 6.8×10^{-5} cm^{2}sec^{-1}. Numerically this gives $\alpha_{\max} = 3\times10^{-1}$ radsec^{-2} for bucket V which has the largest disc separation $D = 5.0\times10^{-2}$ cm, whereas the maximum deceleration in the present experiment is about 5×10^{-3} rad sec^{-2}, with the average even smaller. Furthermore, there is no correlation between the magnitude of angular deceleration and the measured maximum velocity of persistent currents, and we conclude that the critical velocities measured here are not associated with normal-fluid turbulence. Finally, for purposes of comparison we note that in all cases $v_{s,c,l}$ is about an order of magnitude greater than both our experimental and theoretical values.

ANDRONIKASHVILI'S ORIGINAL PERSISTENT CURRENT EXPERIMENT REEXAMINED

Andronikashvili made the initial attempt to observe persistent currents of superfluid helium in 1952 by employing a rotatable stack of discs spaced on a central rod (as in his well-known ρ_n/ρ measurements), but with a thin aluminum shell at the outer radius.[14,15] His channel geometry was thus similar to ours, except that $d \gg D$. Depatie later used very similar buckets to successfully create and observe persistent currents.[6]

In Andronikashvili's experiment the bucket was suspended from a torsion fiber. After rotating the system uniformly ($\Omega \approx 3$ radsec^{-1}) at some temperature slightly below T_λ and then cooling to $T = 1.5\,^\circ$K, the bucket was decelerated to rest. By assuming that the normal fluid would follow the discs and that the additional superfluid, formed in the rotating state from previously rotating normal fluid, would not "see" the discs come to rest, it was hoped that a superfluid persistent current would remain. Then, by heating the bucket and converting ρ_s back into ρ_n, the viscosity of the new normal fluid should cause a transient torque on the bucket and deflect the torsion fiber. However, a null result was obtained. Only small random deflections of about $\frac{1}{30}$ the expected value were observed.

Recently,[15] Andronikashvili reexamined his experiment and offered the following explanation for the null result: At the angular velocity used, the Onsager-Feynman density of vortices is about 6×10^3 vortices cm^2. A long time is required for the decay of these lines after the discs are brought to rest, and the mutual friction due to the relative motion of the vortices (with their normal cores) and the stationary normal-fluid damps out the would-be persistent flow.

We suggest another explanation on the basis of our work, since, as Depatie has shown, persistent currents in buckets similar to Andronikashvili's do exist. It is probable that the design calculations for Andronikashvili's experiment assumed that the Landau critical velocity was pertinent (critical velocities involving vortex lines were then unknown), and thus assumed that the maximum velocity of the expected persistent current would be $v_{s,\max} = R_2\Omega \approx 5.7$ cmsec^{-1}, where R_2 is the outer radius of his bucket. However, our results suggest that for Andronikashvili's $D = 2\times10^{-2}$ cm, $d = 1.0$ cm, a critical velocity $v_{s,c,v}$ due to pinned vortex

lines prevails, giving $v_{s,\max}=v_{s,c,v}\approx 10^{-1}$ cm sec^{-1}. This factor of about 60 may well have resulted in the signal not being seen in an apparatus design with the first value of $v_{s,\max}$ in mind. Again it is emphasized that if the vortex lines remain pinned, then the vortices are at rest at $\Omega=0$, and there is no mutual friction with the stationary normal fluid to cause damping of the superfluid flow.

BUCKET VII

After the data for buckets I through VI had been obtained, bucket VII was constructed with a single large channel such that $D \gg d$. According to (8) the linear velocity at which vortex lines should vanish is $v_s=R\Omega_0=3.5\times10^{-1}$ cm sec^{-1}, but the dissipative critical velocity $v_{s,c,v}$ given by (6) is only 6.6×10^{-4} cm sec^{-1}, so that a large irrotational persistent current is expected at $\Omega=0$. However, the initial data for bucket VII were disappointing. Only small currents were observed and then with large scatter, and there was evidence of spurious angular impulses due to local boiling. This behavior suggested that incomplete destruction of the currents was occurring, and for this reason a different kind of data were taken. Instead of decelerating all the way to $\Omega=0$, currents were also measured over a range of nonzero Ω, and for these data Ω^+ was always considerably greater than both Ω and Ω_0, so that the maximum current relative to the bucket could be expected. Since we now measured the angular momentum L_s of currents relative to the bucket frame rotating at Ω, we expected L_s to fall on the dotted line in Fig. 9. This can be understood by noting that $v_{s,c,v}$ is very small for bucket VII. Thus, there should be no measurable persistent currents relative to the bucket above $\Omega=\Omega_0$. However, as the bucket is decelerated through Ω_0, the vortex lines should vanish, decoupling the superfluid from the bucket and leaving an irrotational persistent current with velocity $v_s=R\Omega_0$ with respect to the laboratory (nonrotating) frame. In the rotating frame of the bucket this relative persistent velocity is $v_s=R(\Omega_0-\Omega)$, and since L_s is proportional to v_s we expect L_s to fall on the dotted line in Fig. 9.

The advantage of measuring L_s at nonzero Ω is that the bucket can be heated to above T_λ, and after the unavoidable transients associated with a large Q_{det} have occurred a final angular velocity $\Omega+\Delta\Omega$ can be measured. Such an approach is not possible for currents measured at $\Omega=0$ (buckets I through VI) since small asymmetries in the magnetic bearing result in a rotational potential well (depth 10^{-2}–10^{-3} ergs) which prohibits complete rotation for small Ω. Instead, slow oscillatory motion then occurs which is superimposed on a drift in the zero of this oscillation. This zero drift is erratic and not completely understood but seems to be associated with the final stages of pumping out the vacuum region. Although the drift is negligible during the time (a few seconds) required to measure $\Delta\Omega$ at $\Omega=0$, it is significant over the period (3×10^2 sec) of oscillation at the bottom of the rotational potential well, and precludes measurements which involve heating the bucket above T_λ and waiting for transients to die out. On the other hand, the success of measurements at nonzero Ω requires a large L_s and small bucket moment of inertia because of the insensitivity of this second method, and is marginally feasible for the currents expected for bucket VII and not at all for buckets I through VI, where $I_s/I\approx10^{-2}$. The data for bucket VII are shown in Fig. 9 and are inconclusive. The large scatter in the data at lower Ω is not understood, and may be due to a flow instability. Also, we cannot rule

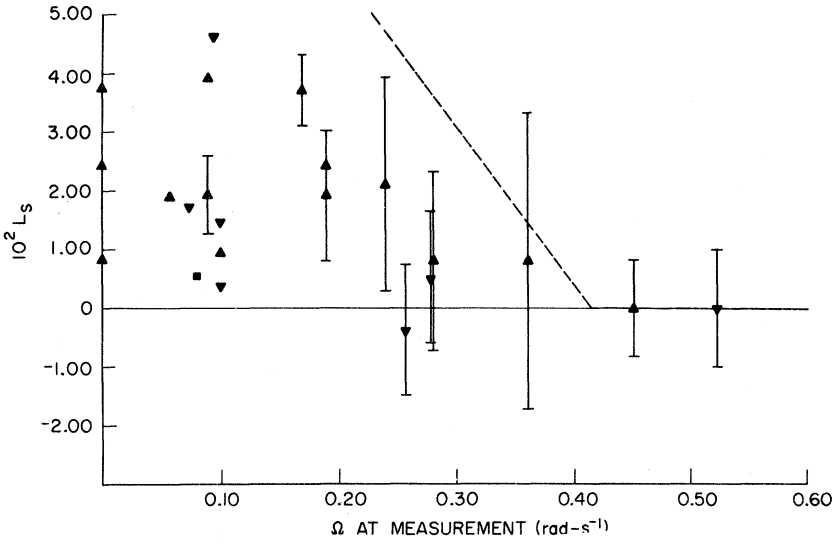

FIG. 9. Bucket VII data. Experimental values of L_s in the bucket's frame of reference are shown as a function of Ω at detection. All currents were made by the Ω^+ method with $\Omega^+ \gg \Omega_0 \simeq 0.41$ rad sec^{-1} and $\Omega^+ \gg \Omega$, so a maximum current was expected at each Ω used for detection. Below 0.41 rad sec^{-1}, L_s was expected to fall on the dotted line; above 0.41 rad sec^{-1}, L_s was expected to be zero. The excessive scatter in the data is not understood.

out normal-fluid turbulence for this bucket. At best, the data are consistent with the combination of a flow instability and a maximum persistent velocity of $v_{s,\max} = 2.6 \pm 0.9 \times 10^{-1}$ cm sec^{-1}, and is therefore not inconsistent with the theoretical value of 3.5×10^{-1} cm sec^{-1}.

CONCLUSIONS

We have made the first direct measurements of the maximum linear velocities of persistent superfluid flow, and find that the measured values are in fair agreement with a simple theory which intimately involves vortex lines. This theory has two ingredients: (i) the dissipative superfluid critical velocity $v_{s,c,v}$ and (ii) identification of Donnelly and Fetter's Ω_o with the superfluid rather than the bucket for metastable persistent flow, with the consequence that if $v_s < R\Omega_o$, pinned vortex lines are unfavorable and are not available for participation in $v_{s,c,v}$. As a result this theory predicts that if $R\Omega_o > v_{s,c,v}$, then at $\Omega = 0$ vortex lines will be absent and the maximum linear persistent flow will be irrotational with a maximum velocity $v_{s,\max} = R\Omega_o$. Similarly, if $R\Omega_o < v_{s,c,v}$, then at $\Omega = 0$ pinned (but curved) vortex lines will be present and the maximum linear persistent velocity will be $v_{s,\max} = v_{s,c,v}$ given by (6).

The bucket channels in which the persistent currents flow are characterized by a height D and width $d = R_2 - R_1$ such that $D \ll d$ in all cases but one (bucket VII). By varying the channel cross section it was possible to obtain either $R\Omega_o > v_{s,c,v}$ or $v_{s,c,v} > R\Omega_o$. For buckets I through VI the values of d and D used gave measured values of $v_{s,\max}$ which are in fair agreement with the values predicted by this theory,[16] and therefore gives strong support to the participation of vortex lines in the superfluid critical velocity. However, the results for bucket VII, which contained a single large channel for which $R\Omega_o \gg v_{s,c,v} \approx$ zero, were puzzling and inconclusive.

In addition we have shown that normal-fluid turbulence was avoided in these measurements, so that the criticism of Van Alphen *et al.* concerning previous critical velocity measurements which agreed with vortex lines does not apply to these measurements. Also, our measured values which agree with a vortex theory are considerably smaller than those predicted by the Leiden formula (8). Finally, we have reexamined the original attempt of Andronikashvili to observe persistent currents, and also his recent new explanation for his null result, and offer a different explanation based on the pinned vortex model for dissipation of an otherwise persistent current.

ACKNOWLEDGMENTS

The author is greatly indebted to Professor J. D. Reppy and Professor C. T. Lane, and to the other members of the Yale low-temperature group for many stimulating discussions.

APPENDIX A

Although we do not know the detailed macroscopic velocity field $v_s(r)$ of the superfluid persistent currents, we can use the approximation $v_s(r) = v_s =$ constant for our geometry. We justify this approximation by comparing the angular momentum per unit length l_s of currents with different possible macroscopic $v_s(r)$ but which have a common maximum velocity $v_{\max}$. We consider the following velocity fields: (i) irrotational, $v_1(r) = (R_1/r)v_{\max}$ for which $l_{s,1} = \pi\rho_s R_1(R_2^2 - R_1^2)v_{\max}$; (ii) solid body, $v_s(r) = (r/R_2)v_{\max}$ for which $l_{s,2} = \frac{1}{2}\pi\rho_s(R_2^3 - R_1^4 R_2^{-1})v_{\max}$; and (iii) constant, $v_3(r) = v_{\max}$ for which $l_{s,3} = \frac{2}{3}\pi\rho_s(R_2^3 - R_1^3)v_{\max}$. Both irrotational and solid body fields are known to occur, while the constant velocity field should also be considered since the pinned vortex critical velocity $v_{s,c,v}$ can limit the macroscopic superfluid flow locally. We note that for our values of R_1 and R_2 the three angular momenta per length are within ten percent of each other for a common value of $v_{\max}$. In view of the precision of earlier experiments concerning superfluid critical velocities,[1] this does not seem to be an unreasonable uncertainty.

APPENDIX B

In order to calculate the lag of the normal fluid with respect to the decelerating bucket, we treat the case of an incompressible viscous fluid of density ρ_n which is entrained between infinite parallel planes of separation D. The initial conditions are that (i) at $t = 0$ both planes and fluid are moving at a constant velocity, and (ii) at $t = 0$ a constant linear deceleration of the planes, $a = \alpha R$, is turned on. Under these conditions the Navier-Stokes equation reduces to the diffusion equation

$$\frac{dv}{dt} = \nu \frac{d^2 v}{dy^2} , \tag{11}$$

where v is the fluid velocity relative to the planes, y is the coordinate perpendicular to the planes, and ν is the kinematic viscosity. A solution to (11) can be obtained by analogy with a calculation for the conduction of heat in a finite rod. Specifically, we use the solution of Carslaw[17] for a finite rod with ends varied in temperature according to $\phi_1(t)$ and $\phi_2(t)$ with an initial temperature distribution $f(x)$ where x is the coordinate parallel to the planes.

The general solution for our case is, in our notation,

$$v(y,t) = \frac{2}{D} \sum_{n=1}^{\infty} e^{-\nu(n\pi/D)^2 t} \sin\left(\frac{n\pi y}{D}\right) \times \left[\int_0^D v_0 \sin\left(\frac{n\pi y'}{D}\right) dy'\right.$$

$$+\frac{n\nu\pi}{D}\int_0^t e^{\nu(n\pi/D)^2\lambda}[1-(-1)^n]\alpha R\lambda\, d\lambda\Big]. \quad (12)$$

We anticipate having to estimate the onset of turbulence by using a critical Reynolds number R_c, where the velocity appearing in R_c is $\bar{v}$, the average velocity across the channel. This is valid for the case of steady flow, but since we have time-dependent motion, we conservatively substitute $v_{\max}$ for $\bar{v}$, where $v_{\max}$ is the maximum relative velocity of the fluid with respect to the planes. Since the deceleration drags the fluid near the planes into motion first, the largest lag is at the center of the channel. Thus, we want to examine

$$v_{\max}(t) = v(0,t) - v(\tfrac{1}{2}D, t)\ , \quad (13)$$

where $v(0,t) = \alpha R t$. The largest relative velocity occurs at $t=\infty$ and, after evaluating (13), is

$$v_{\max} = \alpha R D^2/8\nu\ . \quad (14)$$

We also note that the longest normal-fluid damping time is $D^2/\nu\pi^2$, which is at worst about 5 sec.

*Work supported by the National Science Foundation and the U.S. Army Research Office (Durham).

†Part of a Ph.D. thesis submitted to Yale University.

‡Present address: Physics Department, Massachusetts Institute of Technology, Cambridge, Mass. 02139.

[1](a) R. De Bruyn Ouboter, K. W. Taconis, and W. M. Van Alphen, in *Progress in Low Temperature Physics*, edited by C. J. Gorter (North-Holland, Amsterdam, 1967), Vol. 5, p. 44; (b) also, for a recent general reference on superfluid helium, see J. Wilks, *The Properties of Liquid and Solid Helium* (Oxford U. P., London, 1967).

[2]J. C. Weaver, Phys. Letters 31A, 97 (1970).

[3]J. D. Reppy and D. A. Depatie, Phys. Rev. Letters 12, 187 (1964); James C. Weaver, thesis (Yale University, 1969) (unpublished).

[4]J. Clow and J. D. Reppy, Phys. Rev. Letters 16, 887 (1966).

[5]J. C. Weaver, Rev. Sci. Instr. 42, 275 (1971).

[6]D. A. Depatie, thesis (Yale University, 1965) (unpublished).

[7]R. P. Feynman, in *Progress in Low Temperature Physics*, edited by C. J. Gorter (North-Holland, Amsterdam, 1955), Vol. 1, p. 17.

[8]G. W. Rayfield and F. Reif, Phys. Rev. Letters 11, 305 (1963).

[9]W. I. Glaberson and R. J. Donnelly, Phys. Rev. 141, 208 (1966).

[10]This model was first suggested by J. D. Reppy and worked out by him along with M. J. Stephen and the present author (unpublished).

[11]R. J. Donnelly and A. L. Fetter, Phys. Rev. Letters 17, 747 (1966); A. L. Fetter, Phys. Rev. 153, 285 (1967).

[12]W. M. Van Alphen, G. J. Van Haasteren, R. De Bruyn Ouboter, and K. W. Taconis, Phys. Letters 20, 474 (1966); R. De Bruyn Ouboter, K. W. Taconis, and W. M. Van Alphen, in Ref. 1(a), p. 72.

[13]L. D. Landau and E. M. Lifshitz, *Fluid Mechanics* (Pergamon, New York, 1959), p. 114.

[14]E. L. Andronikashvili, Zh. Eksperim. i Teor. Fiz. 22, 62 (1952).

[15]E. L. Andronikashvili and Yu. G. Mamaladze, in Ref. 1(a), p. 85.

[16]For reasons of sensitivity it is not attractive to attempt measurements for cases with currents limited by still smaller values of $v_{s,c,v}$, since to realize comparable conditions we need $v_{s,c,v} > R\Omega_0$; $v_s \simeq$ constant; $d \ll R$ and $D \ll d$. The net effect of these conditions is to require a larger radius bucket, but since $I \propto R^2$ or worse, $L_s/(I+I_s)$ rapidly becomes too small to be attractive.

[17]H. S. Carslaw, *Introduction to the Theory of Fourier's Series and Integrals and the Mathematical Theory of the Conduction of Heat* (MacMillen, New York, 1906), p. 264.

PHYSICAL REVIEW A VOLUME 6, NUMBER 1 JULY 1972

Renormalized Frequency Shift of Coherent Radiation

Y. C. Lee and D. L. Lin

Department of Physics, State University of New York, Buffalo, New York 14214

(Received 22 November 1971)

The radiative correction to the frequency of the spontaneous radiation from a system of two-level atoms in correlated states is calculated in the resonance approximation. A general prescription for renormalization without explicit reference to plane-wave states is given and used to obtain the renormalized frequency shifts. It is shown that the coherence frequency shift is not affected by the mass renormalization.

It is now well known that the spontaneous radiation from a system of atoms, molecules, or spins in a magnetic field is, in general, quite different from that of an isolated particle, owing to the correlations brought about by the radiation field, which we call the coherence effect. This effect has, in fact, been extensively investigated in superradiance,[1] ray forming,[2] coherent line broadening,[3,4] and also in many other related problems.[5]

Intrinsically associated with the line broadening is a shift of the transition frequency which is normally ignored in most of the previous works.